

# Detection of Finescale Climatic Features from Satellites and Implications for Agricultural Planning

BY ITAMAR M. LENSKY AND URI DAYAN

Local finescale climatic conditions may drive ecological and agricultural systems. For example, local climate contributes to the position of species' range boundaries. With climatic change, the boundaries of species' habitats are expected to shrink or expand along with their extinction or invasion. These finescale climatic conditions are driven by local topography and are referred to here as topoclimate.

Information on the local climate may be obtained from measurements or models. Identification of finescale climatic processes necessitates deployment of a network of dense measurements—an expensive mission that is possible only in restricted areas. An alternative approach to deduce local climates is to apply downscaling methods developed to obtain local-scale surface weather from regional-scale atmospheric variables provided by global circulation models. However these methods are still unable to detect small-scale features due to, *inter alia*, misinterpretation caused by our limited understanding of the multiscale interactions featuring the nature of the atmosphere.

Here we present a method that, for the first time, enables an objective classification of topoclimatic regions from satellite remote sensing. This classification is important because the topoclimate controls,

among other things, the life cycle (phenology) of plants and arthropods. These have clear implications for ecology, agriculture, and epidemiology of vector-borne diseases.

**TOPOCLIMATIC PROCESSES.** The physical processes controlling topoclimatic conditions are affected by the diurnal cycle and local topography. The daily variation in air temperature is governed by incoming solar radiation and outgoing terrestrial radiation from Earth's surface. At nighttime, the net terrestrial radiation (i.e., the difference between the outgoing infrared terrestrial radiation and the incoming atmospheric infrared radiation) is negative, hence cooling the surface. This radiative cooling process is greatly modified by increases of cloud cover, air moisture, wind speed, and turbulence, attenuating the nocturnal rate of cooling. The distance from foothills is another important factor since cooling of surfaces at night may also be locally increased by cool air sliding downslope onto adjacent lowlands from the surrounding elevated terrain. Other effects contributing to radiative cooling are night duration and distance from the attenuating effect of the sea.

**THE SATELLITE DATA AND ANALYSIS.** The steady growth in available remote-sensing data of fine spatial resolution seems to be a promising tool for detecting such topoclimatic features. Over the past years, Earth-observing satellites (EOS) have been used for the measurement of environmental variables relevant to epidemiology and public health, using statistical and classification methods. We analyzed time series of EOS data and used the products of this analysis in order to identify topoclimatic features and their locations. The identification is based on knowledge of the physical processes controlling these

**AFFILIATIONS:** LENSKY—Department of Geography and Environment, Bar-Ilan University, Ramat-Gan, Israel; DAYAN—Department of Geography, The Hebrew University of Jerusalem, Jerusalem, Israel

**CORRESPONDING AUTHOR:** Itamar Lensky, Department of Geography and Environment, Bar-Ilan University, 52900, Ramat-Gan, Israel

E-mail: itamar.lensky@biu.ac.il

DOI:10.1175/2011BAMS3160.1

©2011 American Meteorological Society

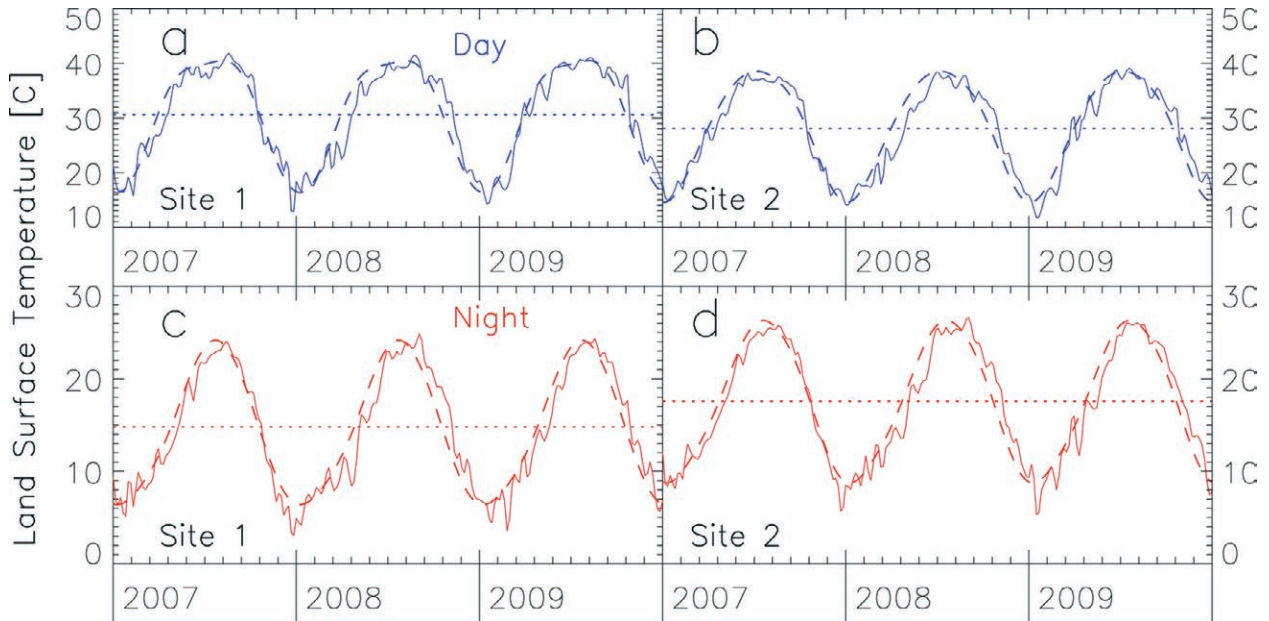


**FIG. 1. Climatological features on a topoclimate scale. LST time series of two pixels from Israel's northern coastal plain for 2007–09: south of Acre (site 1) in panels (a) and (c), and Haifa airport (site 2) in panels (b) and (d). Locations are indicated in Fig. 2. The original day (blue) and night (red) LST time series are displayed in continuous lines, Fourier fit in dashed lines, and the mean LST in horizontal dotted lines. Whereas the mean day LST of both sites are similar (Figs. 1a and 1b), the mean night LST of site 1 (Fig. 1c) is lower than that of site 2 (1d) and the amplitude between winter and summer is larger.**

features. For this purpose we used the freely available preprocessed 8-day average clear-sky Land Surface Temperature (LST) product from the MODerate resolution imaging Spectroradiometer (MODIS) on NASA's *TERRA* satellite. Data from this product from March 2000 are available at <https://wist.echo.nasa.gov/~wist/api/imswelcome>. *TERRA* is a sun-synchronous satellite, which passes over any given point of Earth's surface around 10:30 a.m. and p.m. local mean solar time. The spatial resolution of this product is 0.928 km by 0.928 km, gridded in tiles of 1,200 rows and 1,200 columns in sinusoidal projection. This spatial resolution is "fine" as related to typical standard surface meteorological data, and will be referred here as "finescale."

We constructed a 10-yr time series (2000–09) of the LST product over northern Israel, along the East Mediterranean coast, and applied Temporal Fourier Analysis (TFA) to these time series. Since we are looking at the seasonal cycle, we used the annual ( $\omega_1 = 2\pi/365$  days), biannual ( $\omega_2 = 2\omega_1$ ) and triannual ( $\omega_3 = 3\omega_1$ ) harmonics. The TFA, denoted as  $f_t$ , is the sum of the mean of the time series ( $\bar{f}$ ) and the three harmonics. Each harmonic is described by its amplitude ( $A_i$ ) and phase ( $\phi_i$ ).

$$f_t = \bar{f} + \sum_{i=1}^3 A_i \cos(\omega_i t + \phi_i)$$

Next, detection of finescale climatic features is demonstrated using the mean of the time series ( $\bar{f}$ ) and the amplitude of the annual cycle ( $A_1$ ), which is the cycle contributing most to the seasonal signal. Radiative cooling, a worldwide typical finescale feature, is demonstrated here over irregular terrain ranging from 200 m below sea level to 1,200 m above sea level in northern Israel.

**DETECTING RADIATIVE COOLING.** Figure 1 shows day and night LST time series from two nearby distinct topoclimatic regions, represented by two pixels (sites 1 and 2) on the northern coastal plain of Israel. The elevation of both sites is about 6–7 m above sea level, illustrating the large spatial variability inherent to topoclimatic scales. Whereas the mean day LST of both sites are similar (Figs. 1a and 1b), the mean night LST of site 1 (Fig. 1c) is lower than that of site 2 (1d) and the amplitude between winter and summer is larger, as shown also in Fig. 2 over all northern Israel.

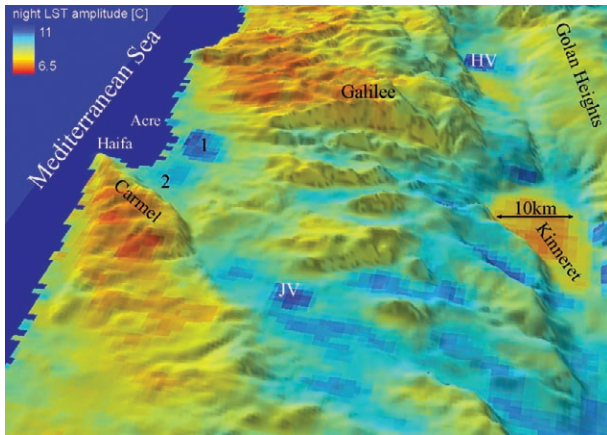


**FIG. 2. Amplitude of the first harmonic (annual cycle) of the night LST based on the same dataset as Fig. 3. Note that all three cold patches of night LST (Fig. 3b) are shown here as large amplitudes between winter and summer (blue patches).**

Though both sites are located near the Mediterranean Sea shore, the diurnal and seasonal cycles are not attenuated by the sea due to prevailing southeasterly offshore winds characterizing winter nights. During such nights, stable atmospheric conditions suppress turbulence, leaving radiative cooling as the major component in the energy budget near the surface. This radiative cooling enhanced by drainage flow from the Western Galilee Mountains is manifested in colder winter night LST in the northern site. Wind flow at the southern site is enhanced by a channeling effect caused by Mount Carmel, leading to weak turbulence in the shallow atmospheric

layers, suppressing radiative cooling (mean winter night turbulence intensity values calculated for both horizontal components were approximately 0.2). Moreover, the mean rain depth differences in these two sites (461 mm for site 1 as compared to 556 mm for site 2) for 8 consecutive years, using a *t*-test for paired samples, confirms the distinct local climate of these nearby sites.

To identify radiative cooling on a larger geographical domain, in Fig. 3 we present maps of the mean day and night LSTs for the northern part of Israel. The mean day LST (Fig. 3a) is largely controlled by the altitude: the Galilee and Carmel Mountains are colored blue, indicating lower temperatures as compared to the warmer lowlands. The cool water of Lake Kinneret (Sea of Galilee) is eminently surrounded by warm valleys. At nighttime (Fig. 3b), the large blue patches represent the cold Galilee mountains and the Golan Heights, whereas the other three isolated blue patches are the Hula Valley in the north (HV), Jezreel Valley in the south (JV), and Zevulun Valley (site 1), all prone to radiative cooling. Figure 2 shows the amplitude of the annual cycle (first harmonic) of the night LST.

The largest amplitude of the night LST can be seen in the three valleys (HV, JV, and site 1), while the smallest amplitudes (colored red) are seen over the Carmel and Galilee Mountains and Lake Kinneret. For a clearer demonstration of the radiative cooling phenomena displayed in Fig. 3b, we show the contribution of the summer (June, July, August) and winter (December, January, February) night LST separately in Fig. 4. The above-mentioned conditions

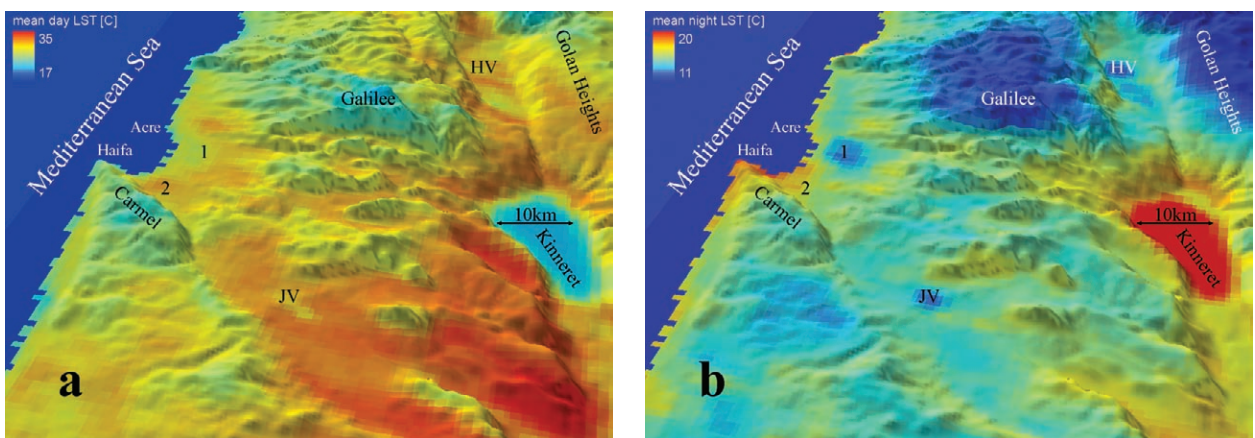


**FIG. 3. Mean LST: (a) day, and (b) night (over the period from Mar 2000 to Dec 2009) for northern Israel. Locations of sites 1 and 2 are indicated. Note the three cold (blue) patches in the night LST in valleys prone to radiative cooling (JV, HV, and site 1).**

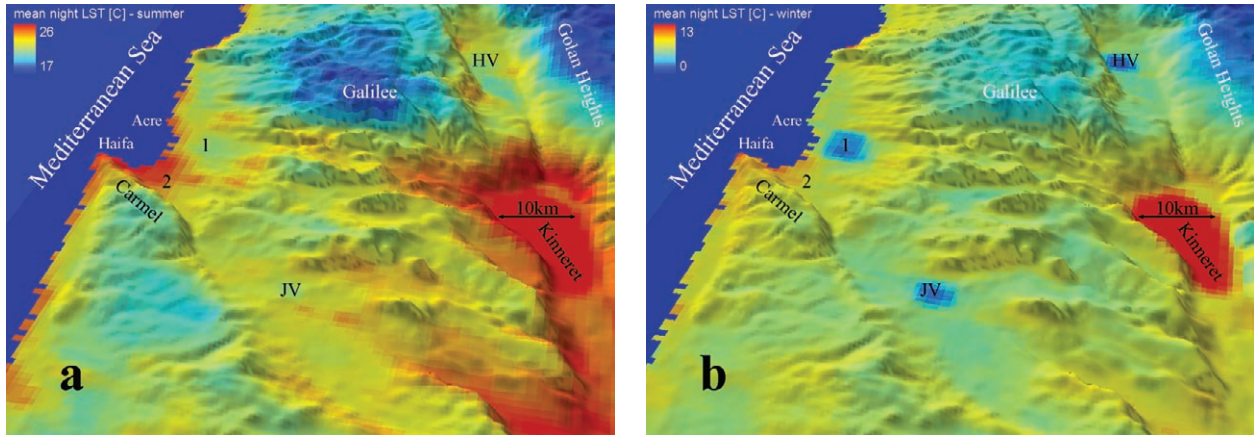


**FIG. 4. Mean LST for (a) summer (JJA) nights, and (b) winter (DJF) nights, based on the same dataset as Fig. 3. It is evident from (b) that the strong signal of the night LST in Figs. 2 and 3b in the three valleys (JV, HV, and site 1) is attributed to low winter night LST (blue patches)—a manifestation of radiative cooling.**

leading to strong radiative cooling are met during the longer winter nights, as evident from the three cold patches in Fig. 4b, for which the mean LST winter nights are significantly colder than that of the Galilee Mountains (1,200 m ASL). Since the dimensions of these patches are of a few kilometers wide, time-series analysis of fine-scale satellite data seems to be the sole objective method to detect and identify these cold patches manifesting topoclimatic scale features.

**IMPLICATIONS FOR AGRICULTURAL PLANNING.** The thermal heterogeneity resulting from the topography shown in Fig. 3 has strong impacts on ecological systems (e.g., biodiversity) and on agriculture (e.g., pest management and crop production). Temperature is the key factor in the development of arthropods and crops. Therefore, questions such as when to plant, whether the crop is developing on time, and when to initiate pest control actions depend on temperature.

Two of the most important external environmental factors that exert great influence on the growth and development of plants are the intensity and duration of the light received by the plant and the temperature of the air and soil around the plant. Knowing the growth stages of sweet corn (*Zea mays* L.), as an example for crops, allows growers to properly time their field operations (e.g., fertilize, irrigation, cultivation, harvest, and pests, weed, and disease control), which can significantly improve yields.

For most plants, phenological development is strongly related to the accumulation of heat or temperature units above a base temperature ( $T_{base}$ )

below which little growth occurs. The value of  $T_{base}$  varies with plant species; for sweet corn,  $T_{base} = 10^{\circ}\text{C}$ . Growing degree days (GDD) is defined as:

$$GDD = \frac{T_{max} + T_{min}}{2} - T_{base}$$

where  $T_{max}$  and  $T_{min}$  are the daily maximum and minimum temperature, respectively.

The height of sweet corn plants, shown in Fig. 5a, was calculated using the accumulated GDD. This figure shows a simulation of corn development as related to local surface temperature. In this case, the planting date of corn was set to 1 May 2005 for the entire region, and its height was checked 110 days after planting. The red patches delineate regions where fastest sweet corn growth is expected. If actual development is slower than the expected development from Fig. 5a, then the possible causes (irrigation, fertilizers, pests) should be examined.

Temperature also controls the developmental rate of many organisms. *Heliothis* is a moth that, like other insects, requires a certain amount of heat to develop from one stage of its life cycle to another (known as physiological time), which is expressed as degree-days ( $^{\circ}\text{D}$ ) similar to the GDD applied for crop development. The value of  $T_{base}$  for *Heliothis* is  $11.5^{\circ}\text{C}$ , and the emergence of the adult *Heliothis* from its pupal case requires  $625^{\circ}\text{D}$ . *Heliothis* is a major agricultural pest worldwide attacking a wide range of food and fiber crops. The direct costs to farmers of crop damage and control measures are enormous—*Helicoverpa* and

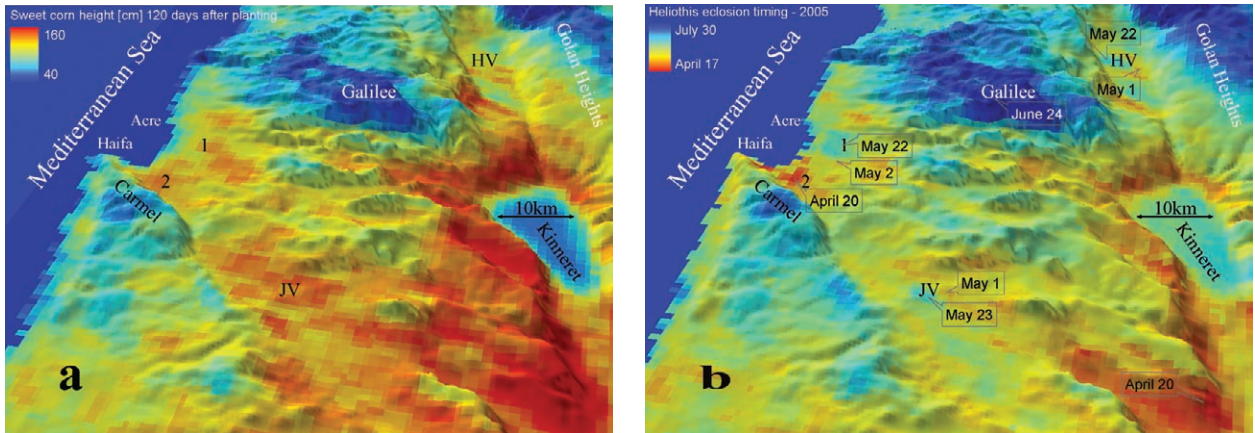


**FIG. 5. Agricultural applications. (a) Simulation of sweet corn growth (height) as related to local land surface temperature. Planting date was set to 1 May 2005 for the entire region. The height was calculated 110 days after planting. The red patches delineate regions where fastest sweet corn development is expected. (b) Ecllosion timing of adult *Heliothis* from its pupal stage for 2005. Note that in the three valleys prone to radiative cooling, ecllosion occurs about three weeks later than in the immediate surrounding lowlands.**

*Heliothis* species account for billions of dollars lost worldwide each year.


Predicting the timing of pest population expansion depends on the climate spatial variability induced by local topography, and can be used to time scouting efforts and pesticide applications. To demonstrate the influence of topoclimate on the timing of the emergence of adult *Heliothis* from its pupal stage at the end of the winter (ecllosion), we use the 2005 LST time series as an example for information that is important for integrated pest management. Figure 5b shows the spatial variability of the day in the year when the adult *Heliothis* population is expected to begin expanding, while taking into consideration only the temperature. The actual population may be controlled by other factors, such as local winds, availability of food, and application of pesticides. While in warm areas, ecllosion of adults occurs in late April (site 2, and the valleys surrounding Lake Kinneret), in the Galilee Mountains it is delayed until late June. In the three cold patches (Fig. 4b), ecllosion is delayed until 20 May—about three weeks later than in the immediate surrounding lowlands. Knowledge of the LST spatiotemporal variability has important indirect climate implications. Pest management is a worldwide issue: despite the large amount of pesticide applied worldwide, pests, insects, weeds, and plant pathogens destroy about 40% of all crops. Here we showed that satellite remote sensing for agrometeorological applications offers an important tool for agricultural planning and management. This new approach is

important in a world of rapidly growing population and need for food supply.

**ACKNOWLEDGMENTS.** This study was supported by the Binational US-Israel Agricultural Research and Development Fund (BARD, IS-4105-08). We thank NASA for the Land Surface Temperature (LST) product from MODerate resolution Imaging Spectroradiometer (MODIS). We convey our gratitude to the two anonymous reviewers for their constructive comments that greatly improved the manuscript.

## FOR FURTHER READING

- Barteková, A., and J. Praslička, 2006: The effect of ambient temperature on the development of cotton bollworm (*Helicoverpa armigera* Hübner, 1808). *Plant Protect. Sci.*, **42**, 135–138.
- Benkova, I., and P. Volf, 2007: Effect of temperature on metabolism of *Phlebotomus papatasi* (Diptera: Psychodidae). *J. Med. Entomol.*, **44**, 150–154.
- Hurrell, J., G. A. Meehl, D. Bader, T. L. Delworth, B. Kirtman, and B. Wielicki, 2009: A unified modeling approach to climate system prediction. *Bull. Amer. Meteor. Soc.*, **90**, 1819–1832.
- Luna, R. E., and H. W. Church, 1972: A comparison of turbulence intensity and stability ratio measurements to Pasquill stability classes. *J. Appl. Meteor.*, **11**, 663–669.
- Luttrell, R. G., 1994: Cotton pest management: Part 2. A US Perspective. *Annu. Rev. Entomol.*, **39**, 527–542.

- 
- Marcus, M., 1999: *Heliothine Moths of Australia. A Guide to Pest Bollworms and Related Noctuid Groups*. CSIRO Publishing, 320 pp.
- McMaster, G. S., and W. W. Wilhelm, 1997: Growing degree-days: One equation, two interpretations. *Agric. For. Meteor.*, **87**, 291–300.
- Merrill, S. C., A. Gebre-Amlak, J. S. Armstrong, and F. B. Peairs, 2010: Nonlinear degree-day models for postdiapause development of the sunflower stem weevil (Coleoptera: Curculionidae). *J. Econ. Entomol.*, **103**, 302–307.
- Pimentel, D., 2009: Pesticides and Pest Control. *Integrated Pest Management: Innovation-Development Process*, R. Peshin and A. K. Dwahan, Eds., Springer, 83–87.
- Scharlemann, J. P. W., D. Benz, S. I. Hay, B. V. Purse, A. J. Tatem, G. R. W. Wint, and D. J. Rogers, 2008: Global data for ecology and epidemiology: A novel algorithm for temporal Fourier processing MODIS data. *Plos ONE*, **3**, e1408.
- Tatem, A. J., S. J. Goetz, and S. I. Hay, 2004: *Terra and Aqua*: New data for epidemiology and public health. *Int. J. Appl. Earth Obs. Geoinf.*, **6**, 33–46.
- Thomas, C. D., 2010: Climate, climate change and range boundaries. *Divers. Distrib.*, **16**, 488–495.
- Williams, M. M., and J. L. Lindquist, 2007: Influence of planting date and weed interference on sweet corn growth and development. *Agron. J.*, **99**, 1066–1072.
- Wilson, L., and W. Barnett, 1983: Degree-days: An aid in crop and pest management. *Calif. Agric.*, **37**, 4–7.
- 
-